BIOCHEMISTRY
including biophysical chemistry & molecular biology

Article

pubs.acs.org/biochemistry

Blue Light Regulated Two-Component Systems: Enzymatic and Functional Analyses of Light-Oxygen-Voltage (LOV)-Histidine Kinases and Downstream Response Regulators

Fernando Correa,[†] Wen-Huang Ko,[†] Victor Ocasio,[†] Roberto A. Bogomolni,[‡] and Kevin H. Gardner*[,†]

[†]Departments of Biophysics and Biochemistry, University of Texas Southwestern Medical Center, Dallas, Texas 75390, United States
[‡]Department of Chemistry and Biochemistry, University of California, Santa Cruz, California 95064, United States

Supporting Information

ABSTRACT: Light is an essential environmental cue for diverse organisms. Many prokaryotic blue light photoreceptors use light, oxygen, voltage (LOV) sensory domains to control the activities of diverse output domains, including histidine kinases (HK). Upon activation, these proteins autophosphorylate a histidine residue before subsequently transferring the phosphate to an aspartate residue in the receiver domain of a cognate response regulator (RR). Such phosphorylation activates the output domain of the RR, leading to changes in gene expression, protein−protein interactions, or enzymatic activities. Here, we focus on one such light sensing LOV-HK from the marine bacterium *Erythrobacter litoralis* HTCC2594 (EL368), seeking to understand how kinase activity and subsequent downstream effects are regulated by light. We found that photoactivation of EL368 led to a significant enhancement in the incorporation of phosphate within the HK domain. Further enzymatic studies showed that the LOV domain affected both the LOV-HK turnover rate (k_{cat}) and K_m in a light-dependent manner. Using *in vitro* phosphotransfer profiling, we identified two target RRs for EL368 and two additional LOV-HKs (EL346 and EL362) encoded within the host genome. The two RRs include a PhyR-type transcriptional regulator (EL_PhyR) and a receiver-only protein (EL_LovR), reminiscent of stress-triggered systems in other bacteria. Taken together, our data provide a biochemical foundation for this light-regulated signaling module of sensors, effectors, and regulators that control bacterial responses to environmental conditions.

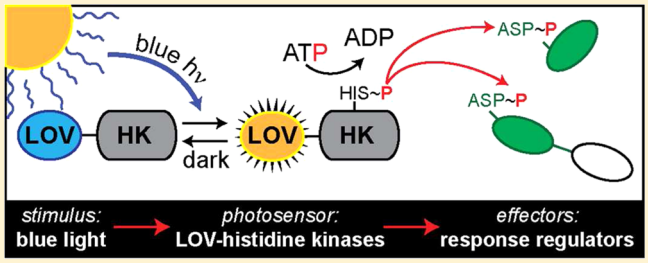

Organisms have developed stimulus-response coupled mechanisms to sense and to adapt to the myriad physical and chemical changes in their surroundings. A common example of such signaling in prokaryotes is provided by phosphorelay systems based on two types of proteins: a sensory histidine kinase (HK) and a downstream response regulator (RR); activation of the former leads to RR phosphorylation that induces cellular responses via changes in downstream gene expression or interactions within a signaling pathway.[1,2] Light is one of the prevalent stimuli sensed by bacteria because of its dual and opposing roles as a vital source of energy and as a potentially damaging factor to intracellular components. As such, a diverse set of photosensory proteins has evolved to allow these organisms to detect and cope with light throughout the UV and visible spectrum.

A prevalent type of blue light photosensor is provided by the light-oxygen-voltage (LOV) domains,[3,4] a subset of the broader family of Per-ARNT-Sim (PAS) group of environmental sensors.[5] These proteins noncovalently bind FMN or FAD in the dark; upon blue light exposure, a covalent adduct is formed between the flavin isoalloxazine C4a position and a nearby cysteine residue. This bond is stable under illumination but spontaneously breaks in the dark with a time scale of seconds to hours.[6,7] Notably, formation of this bond triggers conformational changes at the central β-sheet of the protein that are propagated to a wide array of downstream domains,[8−10] including HKs, HTH DNA-binding domains, phosphodiesterases, and sigma factor regulators (STAS) domains.[3,11] In LOV-containing HKs (LOV-HKs), light exposure typically leads to an enhancement in the overall kinase activity of the protein,[12−14] implicating an important role of these proteins in sensing and responding to light stimulus. While this has been validated for several LOV-HKs,[3,11,12,14−19] the mechanisms that allow LOV domains to control HK activity remain an active topic of investigation. Such information would benefit both basic knowledge of signal transduction in an essential class of sensory proteins while also facilitating the development of optogenetic tools to control complex signaling pathways.

To this end, we used a series of biochemical tools to characterize the enzymatic mechanisms and signaling pathways of the three predicted LOV-HK proteins from the marine bacterium *Erythrobacter litoralis* HTCC2594:[14] EL368, EL346, and EL362. Both EL368 and EL346 undergo light-dependent

Received: May 16, 2013
Revised: June 17, 2013
Published: June 18, 2013

activation of autophosphorylation kinase activity; in contrast, EL362 contains a point mutation within the critical LOV domain, rendering it insensitive to light. Mechanistically, steady state enzymatic analysis of EL368 showed that the observed photoactivation stems from changes in both k_{cat} and K_m parameters upon illumination. *In vitro* phosphotransfer profiling of EL368 and the two other *E. litoralis* LOV-HKs (EL346 and EL362) reveal two downstream targets: a PhyR-type anti-, antisigma RR and a single domain RR. Examination of their biochemical properties and comparison with the genetically identified *Caulobacter crescentus* LovK/LovR stress signaling system[16] suggests that these substrates are homologues of the *C. crescentus* PhyR and LovR proteins, leading us to designate them as EL_PhyR and EL_LovR, respectively. Intriguingly, all three LOV-HKs phosphorylate EL_LovR, while EL_PhyR is targeted more specifically by only EL368 and EL346. This type of signaling network is reminiscent of general stress responses in several alphaproteobacteria,[20,21] particularly via parallels with the *Caulobacter crescentus* pathway where PhyR regulates an operon containing an EL368-homologue and its cognate RR.[16] Altogether, our findings suggest that LOV-HKs may participate in conserved branched transduction pathways in bacteria essential to biological responses to stress.

EXPERIMENTAL PROCEDURES

Cloning, Expression, and Purification of LOV-HK and Response Regulator Proteins. DNA-encoding sequences of the LOV-HK proteins EL368, EL346, and EL362 (NCBI Gene locus tags ELI_02980, ELI_04860, and ELI_07650, respectively) and anti-σ factor (locus tag ELI_10225) were amplified from *Erythrobacter litoralis* HTCC2594 genomic DNA[22] and cloned into the pHis-Gβ1-parallel expression vector.[23] Response regulators (locus tags in Table S1, Supporting Information) were amplified from *Erythrobacter litoralis* HTCC2594 genomic DNA and cloned into pHis-parallel expression vector.[24] Mutants EL368 (C93A) and EL362 (R150G) were generated with QuickChange II XL site-directed mutagenesis kit (Stratagene). *Escherichia coli* BL21(DE3) cells transformed with those vectors were grown at 37 °C in LB media containing 100 μg/mL of ampicillin to an A_{600} of 0.8, then induced overnight at 18 °C by the addition of 0.4 mM isopropyl β-D-thiogalactoside. Cells were harvested, resuspended into 50 mM Tris at pH 8.0 and 100 mM NaCl buffer, lysed by extrusion, and centrifuged at 48,000*g* for 45 min. The supernatant fraction was initially loaded onto a Ni^{2+} affinity column (Chelating Sepharose Fast Flow, GE Healthcare) pre-equilibrated with the above buffer plus 25 mM imidazole. Proteins were eluted using a 25 to 500 mM imidazole gradient and then digested with His_6-TEV protease.[25] Cleaved target proteins were separated from their tags and TEV protease using a Ni^{2+} affinity column; flowthroughs were collected and concentrated (Amicon Ultra, Millipore). A final gel filtration step used HiLoad 16/60 Superdex 75 or HiLoad 26/60 Superdex 200 columns (GE Healthcare), with both columns pre-equilibrated in 50 mM Tris at pH 8.0 and 100 mM NaCl buffer. All protein-containing fractions were analyzed by SDS–PAGE and stored at −20 °C with 50% glycerol (v/v). For the three LOV-HK proteins, all purification steps were performed under dim red light.

Visible Absorption Spectroscopy. UV–vis absorbance spectra of EL368, EL362, and EL362 (R150G) were collected on a Varian Cary 500 spectrophotometer using a quartz cuvette with 1 cm path length. Dark state samples were kept in the dark until data collection; light state samples were generated via flash illumination. Dark state recovery time constants were obtained by monitoring the increase in absorbance at 446 nm at 20 min intervals for 10 h at room temperature. Data points were fitted to a two-phase exponential decay function using the software Prism (GraphPad Software Inc.). All proteins were in 50 mM Tris at pH 8.0, 100 mM NaCl, and 5 mM DTT solutions.

Autophosphorylation Assays. EL368 autophosphorylation reactions were performed at room temperature in 50 mM Tris at pH 8.0, 100 mM NaCl, 5 mM $MgCl_2$, and 5 mM DTT. Reactions were initiated by adding mixtures of radiolabeled [γ-^{32}P]ATP (10–50 μCi, 6000 Ci/mmol, Perkin-Elmer) and cold ATP (0.05–2 mM) in buffer with EL368 (5 μM final concentration) in dark (dim red light) or light (protein sample previously illuminated with photographic flash) conditions. At the appropriate time points, aliquots were removed and quenched into 4× SDS–PAGE sample buffer (50 mM Tris at pH 6.8, 200 mM NaCl, 40 mM EDTA, 0.2% bromophenol blue, 10% (v/v) β-mercaptoethanol, 4% (w/w) SDS, and 20% (v/v) glycerol). Samples were immediately immersed in liquid N_2 and stored at −80 °C before SDS–PAGE analysis. After electrophoresis, the dye front and unincorporated ATP was removed with a razor blade. Subsequently, gels were dried under vacuum at 80 °C for 45 min and exposed for 30 to 60 min to a phosphoimager screen that was subsequently scanned with a Fujifilm FLA-5100 phosphoimager. Band intensity measurements were performed with MultiGauge software (Fujifilm). Initial rates of ^{32}P incorporation were calculated by fitting the first time points to a linear equation; the [ATP] dependence of these rates were fit to a Michaelis–Menten equation to extract K_m and k_{cat} parameters using Prism. EL362 and EL362 (R150G) dark/lit states (5 μM) were autophosphorylated as mentioned above but with 500 μM unlabeled ATP and 50 μCi of [γ-^{32}P]ATP (6000 Ci/mmol, Perkin-Elmer).

Phosphotransfer Profiling. Initially, EL368 or EL346 LOV-HK proteins (10 μM) were autophosphorylated in 50 mM Tris at pH 8.0, 100 mM NaCl, 5 mM $MgCl_2$, 5 mM DTT, 4.5 μCi [γ-^{32}P]ATP (6000 Ci/mmol), and 1 mM ATP for 10 min at room temperature under white light conditions. Response regulators were diluted to 10 μM in the same buffer without nucleotides. Equimolar mixtures of phosphorylated EL368 or EL346 and response regulators (5 μM each) were made and incubated at room temperature for 30 s and 10 min intervals. Samples were treated and imaged for ^{32}P incorporation as described above.

Phosphotransfer Kinetic Measurements. To obtain the phosphotransfer rate of EL368 to the cognate response regulator EL_PhyR (gene locus ELI_10215), 5 μM EL368 in nucleotide-free buffer was mixed with 100 μM EL_PhyR containing 25 μCi [γ-^{32}P]ATP (6000 Ci/mmol) and 1.5 mM ATP. Aliquots were removed at appropriate time points and treated as described above with the exception that the band corresponding to the phosphorylated response regulator was measured. Initial rates for the dark state were obtained with reactions performed under dim red light; lit state EL368 samples were generated by flash illumination prior to the beginning of the reaction and kept under regular white light room illumination. Phosphotransfer of EL362 (5 μM) was done as previously stated for EL368 but with 500 μM ATP and 5 μM of the cognate response regulator EL_LovR (gene locus ELI_07655).

Phosphatase Assay. EL_PhyR phosphatase assays were performed at room temperature in 50 mM Tris, 100 mM NaCl, 5 mM DTT, and 5 mM $MgCl_2$ at pH 8.0. Ten micromolar EL368 was preincubated for 10 min with an equimolar concentration of EL_PhyR and 30 μCi of [γ-^{32}P]ATP. After preincubation 5 mM AMPPNP was added to the reaction to stop further phosphorylation from ATP. For reactions with the EL_LovR (wild type or D52A) proteins, 10 μM of these proteins were added simultaneously with 5 mM AMPPNP. Aliquots were removed at 0.25, 0.5, 1, 2, 5, 10, and 15 min. Samples were treated as described above.

Size Exclusion Chromatography and Multiple Angle Laser Light Scattering. The oligomerization states of EL368 and EL362 were determined with integrated size exclusion chromatography and light scattering (SEC-MALLS). Five hundred microliters of 20 μM EL368, EL368(56−368), EL362, and EL362(R150G) dark/lit samples were injected at 0.5 mL/min flow onto Superdex 75 10/300 or Superdex 200 10/300 analytical columns (GE Biosciences), pre-equilibrated with 50 mM Tris at pH 8.0, 100 mM NaCl, 5 mM $MgCl_2$, and 5 mM DTT buffer. Using a 0.5 mL/min flow rate, these samples were detected postelution using inline miniDAWN TREOS light scattering and Optilab rEX refractive index detectors (Wyatt Technology). All of the procedures were performed at 5 °C. Data analyses and molecular weight calculations were carried out using the ASTRA V software (Wyatt Technology). The same approach was also used to study the complex of the EL_PhyR response regulator and its anti-σ factor. Five hundred microliter samples containing EL_PhyR (30 μM) and anti-σ factor (40 μM) individually or mixed were applied onto Superdex 75 10/300 in line with MALLS pre-equilibrated with the above-mentioned buffer. To study the interaction with the phosphorylated state of response regulator, EL_PhyR by itself or mixed with anti-σ factor was incubated with 0.5 μM EL368 and 2 mM ATP for 30 min prior to injection.

RESULTS

Characterization of Light-Dependent Enzymatic Activity. In addition to a conventional HWE-type HK domain,[26] EL368 contains an N-terminal LOV domain, conferring kinase activation upon blue light exposure.[14] Measurements of the autophosphorylation activity of EL368 using [γ-^{32}P]ATP as substrate in the dark and light show that the protein is approximately four times more active in the lit state (v: 0.007 ± 0.001 s^{-1}) than in the dark (v: 0.002 ± 0.001 s^{-1}) (Figure 1a,b). Changes in kinase activity upon light illumination have also been reported for other natural LOV-HKs[12−14] along with an engineered variant of FixL,[27] clearly indicating that light-induced conformational changes in the LOV domain can allosterically affect the overall activity of the HK domain. However, the underlying mechanisms of such regulation remain unclear. In a very simplistic enzymatic model, the sensor domain could influence overall enzyme activity through changes in the Michaelis constant for various substrates (K_m), V_{max}, or a combination of both. To address which of these enzymatic parameters are affected by illumination, we determined the net kinase activity of EL368 at varying concentrations of ATP. Figure 1b shows that the autophosphorylation reaction catalyzed by the enzyme supports a classical Michaelis−Menten kinetics mechanism in both conformational states. Upon activation, the enzyme presents a four times overall increase in its catalytic rate (V_{max}(dark), 0.002 ± 0.0001 s^{-1}; V_{max}(lit), 0.009 ± 0.0005 s^{-1}). However, there is a slight but measurable decrease of affinity for ATP in the lit state (385 ± 52 μM) in comparison to that in the dark state (131 ± 31 μM). Similar ATP affinities have been reported for other HKs.[28−31]

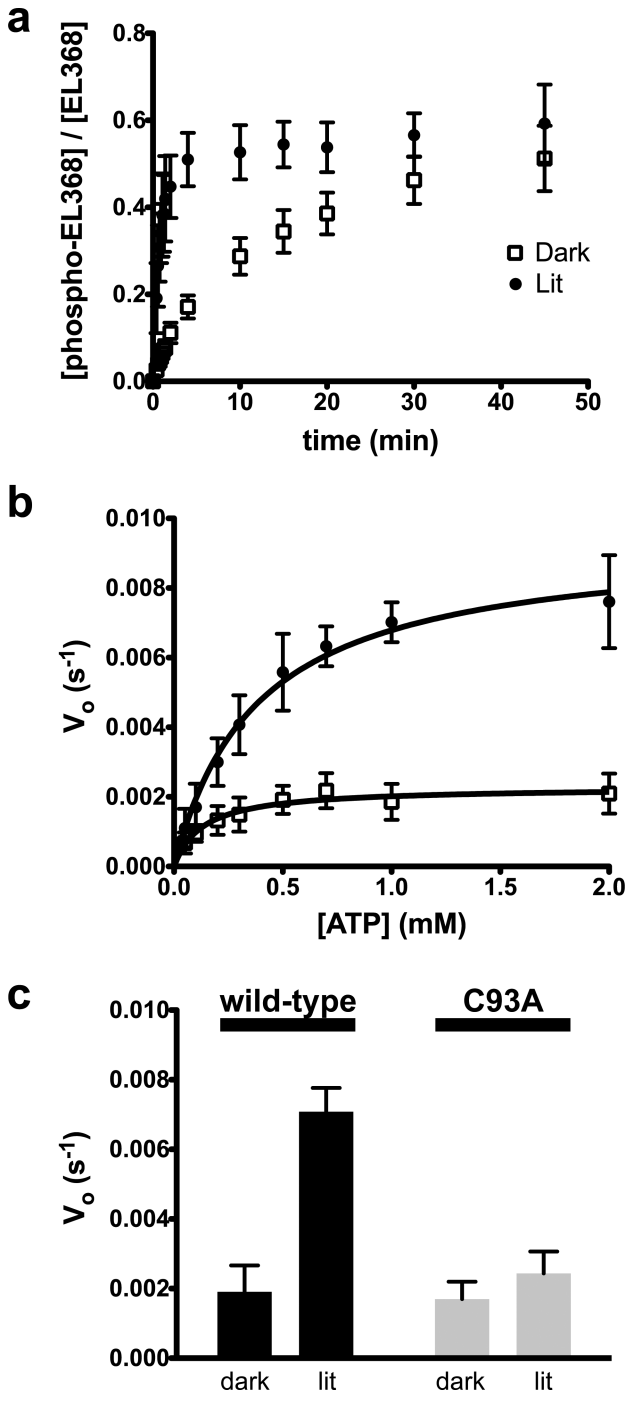

Figure 1. Light enhances the phosphorylation activity of EL368. (a) Time course of phosphate incorporation into EL368 either in dark or white light conditions. Upon light exposure, the enzyme has a higher kinase activity and achieves steady state equilibrium more quickly than the dark state. (b) Initial velocities obtained at different ATP concentrations were fit to a Michaelis−Menten equation (black line). (c) EL368 (C93A) demonstrates that kinase activity observed in the dark state does not arise from residual cysteinyl-flavin adduct formation.

dx.doi.org/10.1021/bi400617y | *Biochemistry* 2013, 52, 4656−4666

One practical issue for measurements of dark state kinase activity is the very slow photorecovery to the dark state observed for this enzyme (~2 h, Figure S1, Supporting Information), which would lead to the accumulation of lit state conformers upon incidental exposure to light. While we took reasonable steps to avoid such exposure, such artifacts could lead to aberrantly high background levels of activity in such phosphorylation assays. To rule this out, we engineered a mutant version (C93A) that binds to flavin but cannot form the cysteinyl adduct. As expected, the mutant displayed a dark state activity (ν: 0.002 ± 0.0005 s^{-1}) comparable to that of the wild-type (ν: 0.002 ± 0.001 s^{-1}) and was only minimally affected by light (ν: 0.002 ± 0.001 s^{-1}) at 1 mM ATP (Figure 1c). Low levels of dark state phosphorylation have also been reported in other LOV-HK systems.[12−14]

LOV Domain Stabilizes Dimeric Conformation. Most HKs studied to date function as dimers, with *cis*- or *trans*-autophosphorylation between subunits of the oligomer.[28,32−34] To examine whether EL368 also operates as a dimer, we took advantage of the long-lived lit state (~2 h) SEC-MALLS to examine the solution oligomerization state of the protein in the dark and light. Results demonstrated that EL368 is primarily a very stable and light-independent dimer in solution (Figure 2).

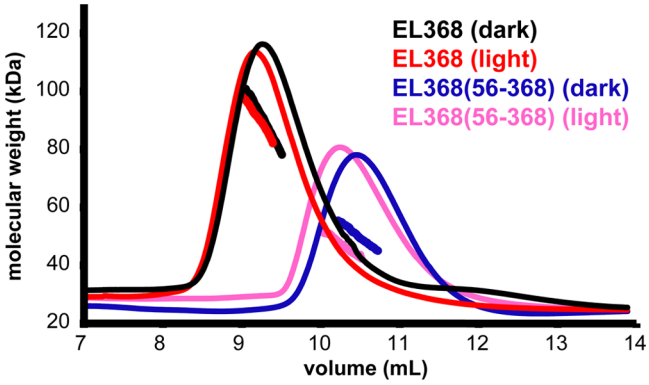

Figure 2. Dimeric solution structure of EL368 is stabilized by elements located N-terminal of the LOV domain. SEC-MALLS traces correspond to full length EL368 (black, dark state; red, light) and EL368(56−368) (blue, dark; magenta, light); dRI traces from the Optilab rEX are shown as solid lines, plotted on the same relative scale, while MALLS-derived mass distributions are plotted as individual points. Full length EL368 is dimeric regardless of illumination, as SEC elution profiles and mass distributions are unaffected by light (apparent MW ~90 kDa at the center of the peak, compared to the monomer MW of 41.4 kDa). Removal of 55 residues prior to the predicted LOV domain generates EL368(56−368) and destabilizes the dimer (apparent MW ~50 kDa at the center of the peak, compared to the monomer MW of 35.2 kDa).

In addition, the minor changes in the elution profile between light and dark conditions suggest that there are no drastic changes in the shape of the enzyme upon activation, in agreement with data reported for the *C. crescentus* homologue LovK.[35]

Secondary structure predictions of EL368 by Jpred[36] indicates that the N-terminal LOV domain is preceded by an additional 56-residue-long region (Figure S2, Supporting Information). Previous studies of other LOV domains have demonstrated that such additional regions can affect photocycle lifetime and oligomerization state,[35,37] leading us to examine their influence in EL368. To do so, we constructed a truncated form of the protein, EL368(56−368). While removal of that segment did not affect the binding to flavin or solubility of the molecule, SEC-MALLS showed that this deletion affected the protein oligomerization state by biasing it toward lower molecular weight (Figure 2). The molecular weight distributions obtained for dark and lit samples suggest that the protein eluted as a mixture of monomers and dimers, with minimal light-dependent effects.

Light Regulated Two-Component Signaling: Identification of Target Response Regulators and Influence of Light Stimulus on Phosphotransfer. Two-component systems are often composed of HKs and RRs found in operons, where they usually form an exclusive phosphotransfer pair. Nevertheless, HKs can be found as "orphans" without candidate RRs nearby in the genome, complicating identification of cognate pairs from the sequence alone.[38,39] Analysis of the *E. litoralis* genome[22] shows that EL368 is encoded as an orphan HK, with the nearest predicted RR over 80 kb away. To further characterize the influence of light stimulation at the phosphotransfer step and suggest a functional role for EL368, we proceeded to identify RR substrates using phosphotransfer profiling. This technique, based on comparisons of the ability of HKs to phosphorylate candidate RRs, takes advantage of the *in vitro* kinetic preference HKs exhibit for their *in vivo* cognate RR.[40]

The *E. litoralis* genome is predicted to encode 23 RRs[41] (Table S1, Supporting Information), 21 of which we successfully expressed in *E. coli*. Twelve of these proteins expressed as full-length constructs; the other 9 were expressed as isolated receiver domains. This approach, which considerably increased the total yield of soluble protein compared to the full-length forms, takes into consideration the fact that the receiver domain defines the complex specificity and phosphotransfer catalysis.[40] We were unable to obtain sufficient quantities of two proteins for further analysis, as they either went into inclusion bodies (ELI_11255) or failed to express (ELI_11920). With these reagents in hand, *in vitro* profiling of EL368 in a very short time scale (30 s) shows that the enzyme efficiently phosphorylated EL_LovR and EL_PhyR (Figure 3a). Extension of the reaction to 10 min allowed the protein to phosphorylate 4 additional response regulators at lower levels, although these may reflect nonspecific cross-talk given the prolonged incubation time[40] (Figure 3b).

In addition to EL368, *E. litoralis* also contains two other LOV-HKs: EL346[14] and EL362 (*vide infra*). The former one is also predicted to be an orphan HK; therefore, we performed the same biochemical mapping scheme. Interestingly, EL346 demonstrated a kinetic preference for the same two RRs initially recognized by EL368 (Figure S3a, Supporting Information; summarized in Figure 3c). Nevertheless, in a longer reaction time point, it phosphorylated only one additional substrate (ELI_09195) (Figure S3b, Supporting Information). EL362 exhibited a different specificity and several other unique properties, discussed below.

To address whether a light stimulus would affect phosphotransfer as well as autophosphorylation, we conducted kinase assays in the dark and light with mixtures of EL368 and its substrates (1:20 ratio). These experiments utilized EL_PhyR as a substrate, as EL_LovR exhibited substantial phosphatase activity (*vide infra*). Following the same trends observed for the autophosphorylation, the amount of phosphorylated RR in the light state was higher than that in the dark state (ν (dark), 0.001 ± 7 × 10^{-5} mol RR (mol kinase)$^{-1}$ s^{-1}; ν (lit), 0.0080 ±

dx.doi.org/10.1021/bi400617y | *Biochemistry* 2013, 52, 4656−4666

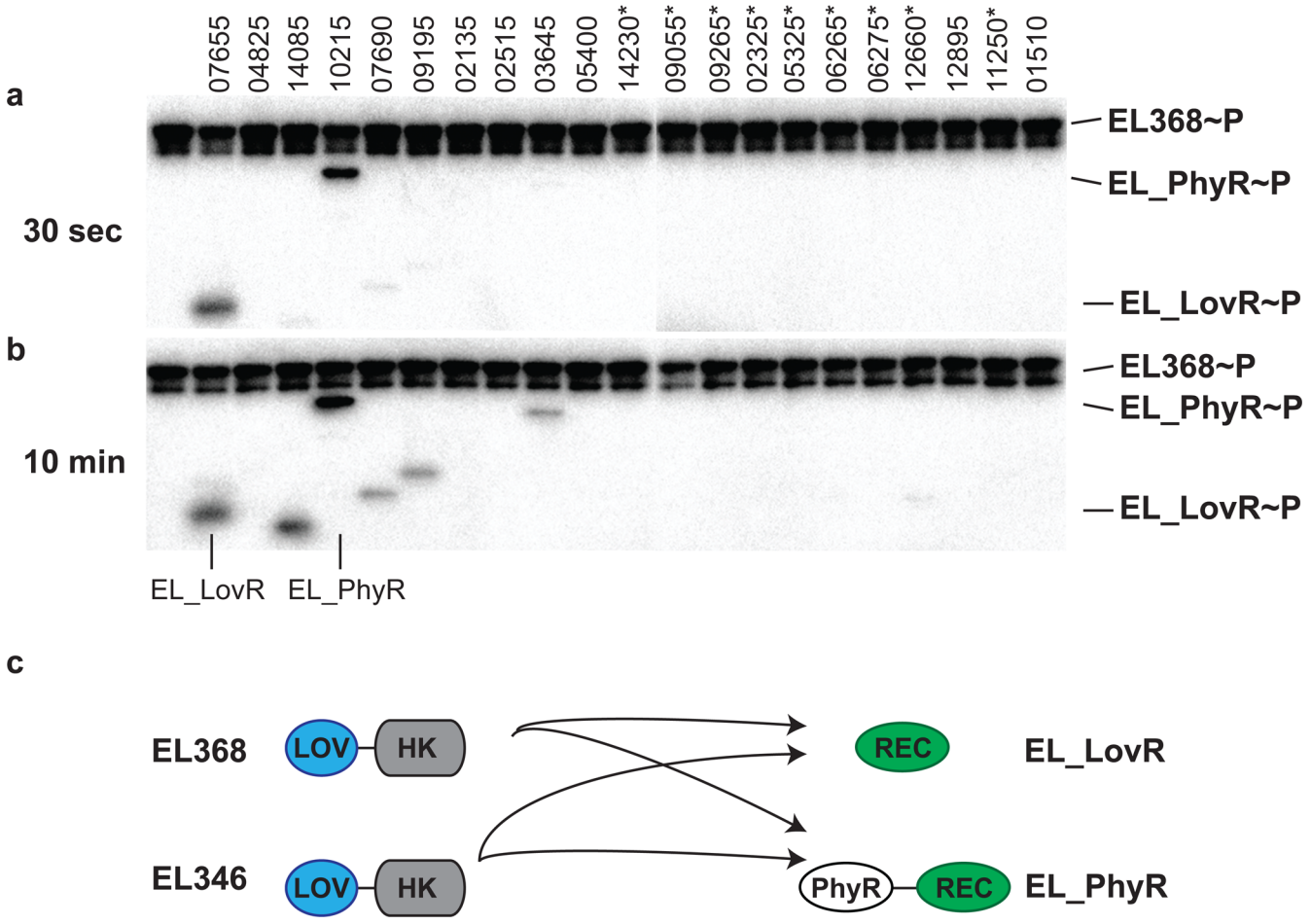

Figure 3. Phosphotransfer profiling of EL368. HK was profiled against 21 RR of *E. litoralis* with phosphotransfer reaction times of 30 s (a) and 10 min (b). In the longer time reaction, several RRs are phosphorylated by the enzyme; however, in a much shorter time point only two kinetically preferred protein substrates (EL_PhyR and EL_LovR) are phosphorylated. Asterisks (*) indicate RR fragments containing only the receiver domain as described in Table S1 (Supporting Information). For optimum resolution, this SDS−PAGE gel was run longer than the comparable gels shown in Figures 4 and 6; EL368 appears as a doublet here as a result. (c) Schematic summary of phosphorylation patterns among the EL368 and EL346 LOV-HK proteins and their RR substrates.

3×10^{-4} mol RR (mol kinase)$^{-1}$ s^{-1}), suggesting that the control exerted by photoactivation primarily affects the levels of phosphorylated HKs that in turn lead to an increase in the population of phosphorylated RRs (Figure 4).

EL368 Controls a Transduction Cascade Involving an σ/Anti-σ Interaction System. To initially suggest potential functions of the two LOV-HK substrates, we used a bioinformatics approach with Hidden Markov Model domain identification implemented by Pfam.[42] This revealed that EL_PhyR combines a C-terminal REC domain with a N-terminal σ factor-like domain, analogous to the PhyR response regulator. PhyR itself is found in an operon with genes for σ and anti-σ factors and a very conserved upstream promoter consensus sequence with −35 (GGAACC) and −10 (CGTT) elements.[20,21,43−45] Under stress conditions, PhyR is activated and binds to the anti-σ factor, increasing the number of free σ subunits that may bind to DNA leading to the transcription of target genes.[20] Notably, the chromosomal region of EL_PhyR shows that it has a arrangement similar to that of the PhyR regulon (Figure 5a), reinforcing the analogy between these proteins.

To test the hypothesis that EL_PhyR may serve as a PhyR homologue, we examined a critical function: binding of phospho-EL_PhyR to the predicted anti-σ (ELI_10225) by using SEC-MALLS experiments with mixtures of both proteins. To generate active RR, we added very small amounts of EL368 (0.5 μM) and ATP (1 mM) prior to the injection onto the system. Phosphorylation did not trigger any drastic change in oligomerization state or shape of ELI_10225, which remains monomeric (Figure 5b); the anti-σ was also monomeric in solution. When both proteins were incubated together, we observed an interaction between the two only when the RR was activated, as demonstrated by a shift in elution volume to 10.6 mL and increase in molecular weight corresponding to the formation of a 1:1 heterodimer of EL_PhyR (MW ∼28 kDa) and ELI_10225 (MW ∼6.4 kDa). We note that a minor population of the inactive RR is also capable of forming some complex with the anti-σ (gray line, 9.8 mL), but differences in both the efficiency of forming this complex and its SEC elution volume suggest that this minor complex substantially differs from the dimer formed by activated protein.

The second substrate, EL_LovR, is annotated by Pfam analysis[42] as a single domain response regulator containing only a REC domain (SDRR). These molecules serve several roles in signaling pathways, from forming protein complexes with downstream elements to serving as phosphate sinks that

dx.doi.org/10.1021/bi400617y | *Biochemistry* 2013, 52, 4656−4666

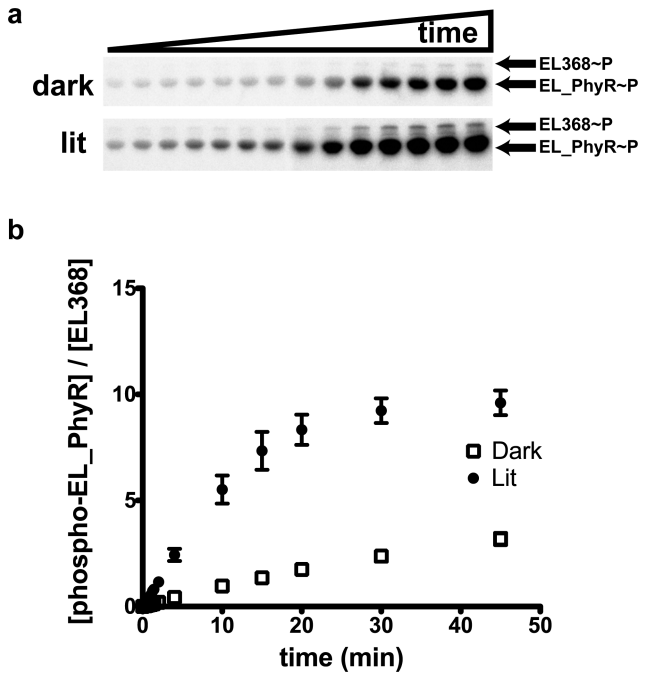

Figure 4. Influence of light on the EL368 phosphorylation of the EL_PhyR substrate. (a) Time course of EL_PhyR by EL368 under dark and light conditions. (b) Quantitation of phosphorylation levels observed in panel a. As observed in the autophosphorylation reaction, light stimulates the phosphorylation activity of the enzyme. The linear phase of the curves (up to 55 s) was used to calculate the initial rates of phosphotransfer.

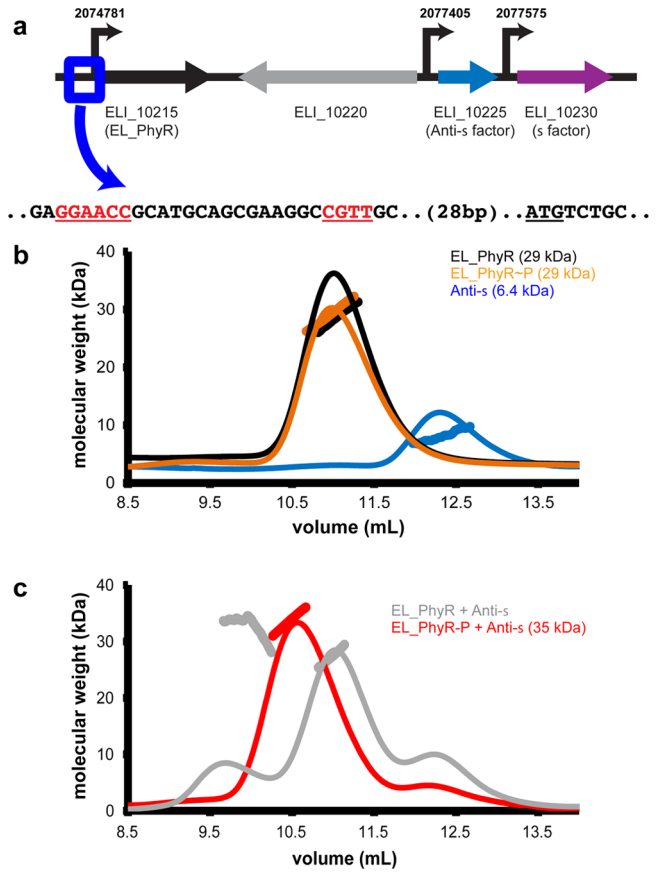

Figure 5. EL_PhyR binds to an anti-σ factor upon activation. (a) Top: Representation of the chromosomal region of EL_PhyR gene. Arrows indicate open reading frames for response regulator EL_PhyR (phyR-like) and anti-σ and σ factors. The coordinates to the initiation codon of each gene are indicates by curved arrows. Bottom: DNA sequence of the 5′ region of the EL_PhyR gene, the putative promoter sequence (red), and the initial residues of the protein. (b) SEC-MALLS results of the isolated versions of the inactive and active forms of EL_PhyR and the anti-σ factor. (c) SEC-MALLS data of combinations of inactive EL_PhyR and anti-σ compared with a mix of the activated EL_PhyR/anti-σ. Changes in the elution volumes and MW distributions of mixtures of EL_PhyR and anti-σ factor show the binding of the two proteins when the response regulator is phosphorylated. Phosphorylated state of the response regulator was generated by adding it to EL368 and ATP and incubating by 30 min at room temperature before injecting in a Superdex 75 10/300GL column. dRI and MW data are shown as described in Figure 2.

modulate pathway activity.[41,46] The combination of EL_LovR and the PhyR homologue EL_PhyR is reminiscent of an analogous stress response system identified in *C. crescentus*.[16] In this system, the SDRR is proposed to act as a phosphate dump based solely on genetic approaches; to provide a biochemical validation for this model and demonstrate its function, we assayed the effects of EL_LovR on the stability of the EL_PhyR~P complex. To do so, we preincubated EL368, [γ-^{32}P]ATP and the EL_PhyR substrate under illumination, efficiently generating the EL_PhyR~P complex, before stopping further kinase activity by adding an excess of nonhydrolyzable AMPPNP. Aliquots taken from this reaction afterward show that the EL_PhyR~P complex is normally stable over the 15 min duration of the assay (Figure 6a). However, when the SDRR is added simultaneously with AMPPNP, we instead see a rapid decrease in EL_PhyR~P accompanied by a transient accumulation of EL_LovR~P (Figure 6b), followed by its rapid dephosphorylation. These data are consistent with EL_LovR serving as a phosphate sink that can rapidly deactivate the EL_PhyR by promoting phosphate turnover. This activity requires the phosphoaccepting D52 residue within the SDRR; mutation to alanine greatly slows these effects while dramatically lowering phosphorylation levels (with low residual phosphorylation likely occurring on nearby residues[47]) (Figure 6c). Taken together, our data suggests that the HK-PhyR-SDRR signaling module reported by genetics in *C. crescentus* can be reconstituted *in vitro* with these *E. litoralis* proteins.

EL_LovR Forms a Two-Component System with a "Blind" LOV Histidine Kinase: Nonflavin Binding Protein Has Impaired Kinase Activity. Analysis of the chromosomal region near EL_LovR revealed another LOV-HK (ELI_07650, named here as EL362) located 18 bp upstream of the RR, suggesting that they might both be located in a shared operon. Phosphotransfer assays confirmed that the enzyme could indeed use EL_LovR as a substrate (Figure S4, Supporting Information); comparable assays with EL_PhyR and an unrelated response regulator showed no phosphorylation (Figure S4, Supporting Information). Interestingly, EL362 also appears to contain a LOV domain based on the presence of the highly conserved GRNCRFLQ motif characteristic of the LOV family[11] (Figure S5, Supporting Information). Nonetheless, we were unable to demonstrate flavin binding to the purified recombinant EL362 protein. This was explained by the presence of an unusual Arg residue at the position of a normally conserved glycine within the Iβ strand of the putative LOV domain (Figure S6, Supporting Information). We have confirmed that the mutation which generates the Arg 150

dx.doi.org/10.1021/bi400617y | *Biochemistry* 2013, 52, 4656−4666

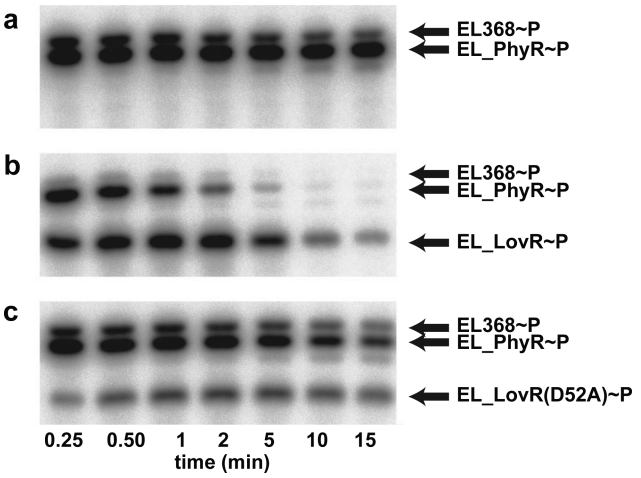

Figure 6. Presence of EL_LovR induces phosphate loss of EL_PhyR. (a) Phosphatase assay of EL_PhyR after phosphotransfer by EL368, demonstrating that phosphorylated EL_PhyR is stable up to 15 min. (b) EL_PhyR rapidly loses phosphate when incubated with unphosphorylated EL_LovR. (c) The phosphoaccepting Asp52 residue is involved in the phosphate turnover of EL_PhyR, as shown by the reduced efficiency of EL_LovR D52A in this process.

residue was found within DNA isolated from strains regrown in our laboratory, as well as being present in the original genomic sequencing data. A homology model of this domain clearly shows that the large Arg side chain would protrude directly into the flavin binding site, blocking chromophore binding (Figure 7a). To confirm this hypothesis, we generated a EL362-(R150G) mutant which reverts this position to the most abundant residue among LOV domains. This change restores both flavin binding and LOV photochemistry to EL362 (Figure 7b), as exhibited by illumination triggering the expected loss of absorbance near 450 nm and subsequent dark state recovery over approximately 3 h. Re-establishment of the flavin binding restored photosensitivity to the kinase activity: dark and lit state samples of EL362(R150G) showed autophosphorylation rates of $0.008 \pm 7 \times 10^{-4}$ s^{-1} vs $0.010 \pm 7 \times 10^{-4}$ s^{-1} (Figure 7c). Notably, both of these levels are higher than those of the wild-type enzyme ($0.001 \pm 1 \times 10^{-3}$ s^{-1}, unaffected by illumination).

We anticipate that these changes in the LOV domain substantially change the domain structure; given their corresponding perturbations of kinase activity, we asked if they affected the EL362 oligomerization state as seen for EL368 (Figure 2). SEC-MALLS experiments showed that wild-type EL362 eluted as a mixture of monomers and higher order oligomers, while the mutant eluted primarily in larger complexes. However, different from EL368, photoexcitation of EL362(R150G) shifted the elution profile in comparison to its dark state (Figure 7d), suggesting a relatively large conformational change. Taken together, EL368(56−368) and EL362 show different ways in which LOV structure is essential to the activity of the HK domain.

DISCUSSION

LOV domains are a widespread group of photoswitches that regulate diverse effectors using light-driven allosteric changes.[3,11,15] These processes have been studied in several systems, particularly the phototropin class of light-regulated serine/threonine kinases in plants. In these proteins, illumination triggers LOV domain conformational changes that disrupt and unfold a C-terminal "Jα helix", subsequently stimulating kinase activity.[8,9] Some LOV-containing proteins appear to work through comparable light-induced release of helical elements, often leading to dimerization;[48,49] others alter the conformations of preformed dimers.[50] Given the diversity of possible mechanisms and targets, it is important to understand how LOV domains control a variety of effectors, particularly given open questions about the natural regulation of several of these groups (e.g., histidine kinases).

Here, we provide some biochemical insight into the mechanism of this regulation, showing that illumination activates EL368 via a dual effect, both enhancing the turnover rate for the kinase activity while slightly decreasing the affinity of the protein to ATP (Figure 1b). The best-developed mechanistic model for how such regulation might be achieved is based on data from YF1, an engineered LOV-HK protein containing a LOV domain fused onto a HK that is normally controlled by a gas-responsive PAS domain.[51−53] This model suggests that light-induced conformational changes at the sensory domain are transmitted to the HK domain through movements in the intervening coiled-coil linker between them, similar to that in HAMP domains that often couple sensory and catalytic domains in HKs. Recent crystal structures of both YF1[53] and a natural PAS-HK protein[54] bolster support for this regulatory model.

We believe that EL368 supports the above-mentioned model for two reasons: (i) the presence of coiled coils predicted by the COILS server[55] to be located between V163-R223 to form a DHp domain (Figure S2, Supporting Information); and (ii) the presence of a stable LOV dimer interface, which may provide the anchor point needed to trigger the rotational change. Experimental support for this is provided by EL368(56−368) (Figure 2) and EL362 (Figure 7), which have LOV domains affected by truncation or the lack of chromophore binding and correspondingly lower amounts of dimer in solution.

Turning from HK regulation to the subsequent downstream targets, we note that the exciting discovery of prokaryotic LOV photosensory proteins with bioinformatic and biochemical methods[3,11,15,16,56] has significantly preceded their functional characterization. To date, only a few of these have had assessed biological roles: several histidine kinases (LovK,[12] BM-LOV-HK,[14] R-LOV-HK,[19] Xac-LOV-HK[17]) along with the EL222 DNA binding protein[57] and the antisigma antagonist YtvA.[58] Here, our investigations of EL368 and two other LOV-HK proteins add to this list, through the use of unbiased phosphotransfer profiling to identify the kinetically preferred downstream targets of these enzymes. Our data reveal that the three enzymes present a remarkable kinetic preference for the same RR (EL_LovR), which is a potential cognate pair with EL362 based on sequence proximity (Figures 3, S3, and S4 (Supporting Information)). EL368 and EL346 also had a kinetic preference for one additional substrate, EL_PhyR (Figures 3 and S3 (Supporting Information)).

Such a "branched" signaling pathway, achieved by multiple enzyme/substrate pairings at the same step, facilitates more complex network behavior than otherwise possible from exclusive links. The biochemical[59] and structural[34,60,61] bases of HK/RR specificity in a two-component pair is defined by residues located near the phosphorylated histidine within the HK DHp domain and mostly by residues in the RR α1 helix. Inspection of EL_LovR and EL_PhyR sequences show that they share similar α1 helices compared to the other *E. litoralis*

dx.doi.org/10.1021/bi400617y | *Biochemistry* 2013, 52, 4656−4666

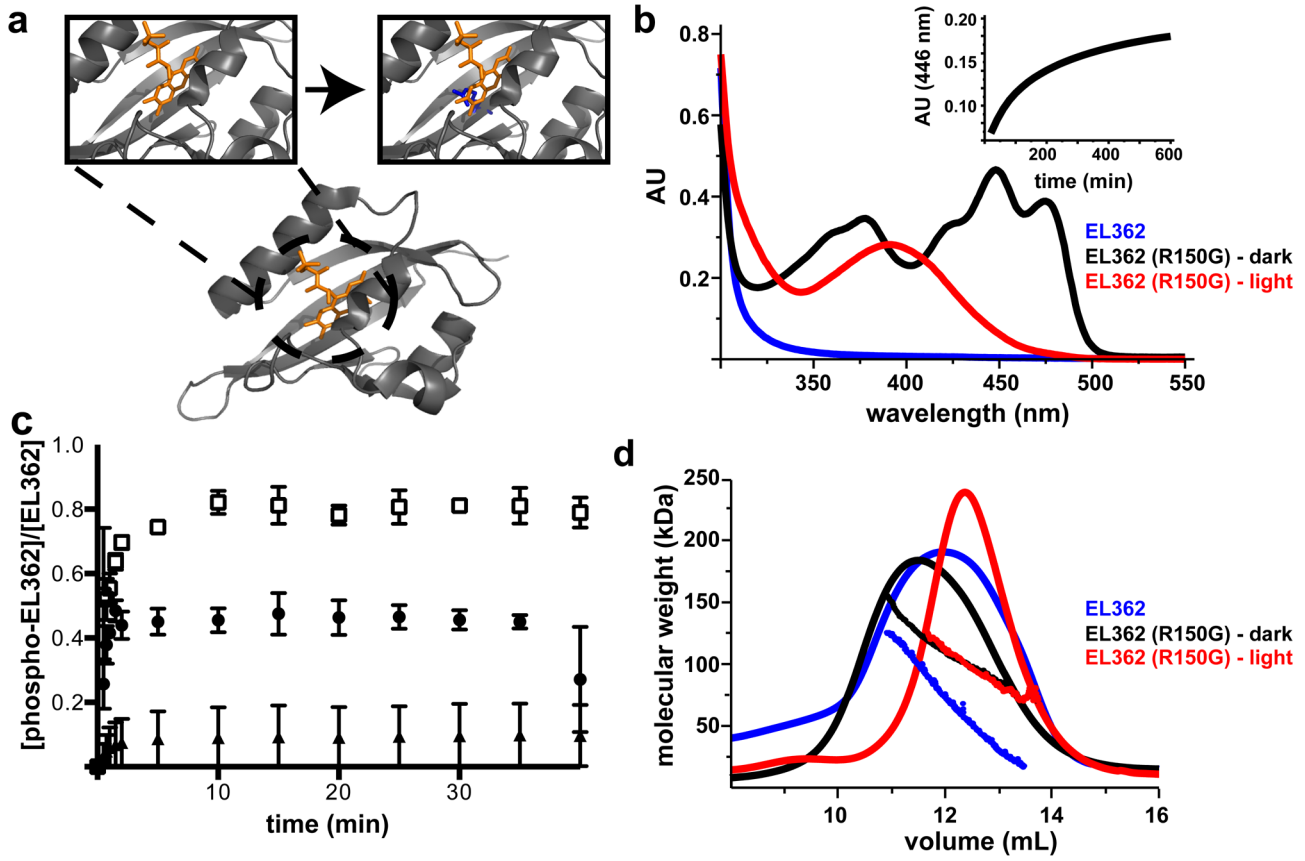

Figure 7. Biochemical characterization of EL362: a blind LOV-HK protein. (a) Predicted effects of R150 residues within the EL362 LOV domain. Bottom center: Structure of a typical LOV domain (*Arabidopsis thaliana* phototropin 2 LOV2 = Atphot2 LOV2, PDB ID 4EEP[62]) showing the location of the internally bound flavin chromophore. Top left: Expansion of the Atphot2 FMN binding site. Top right: Homology model of the predicted site of FMN binding from EL362, superimposing the predicted location of Arg 150 with the FMN bound as seen in other LOV domains. (b) UV−visible absorption spectra of EL362 and EL362 (R150G). The EL362 (R150G) spectrum displays the characteristic vibronic structure of a bound flavin. Upon white light illumination, the flavin undergoes covalent adduct formation. EL362 does not present any spectrum signature indicating the presence of an attached flavin cofactor. EL362 (R150G) photorecovery monitored at 446 nm shows that it undergoes a photocycle after illumination with a dark state recovery that takes approximately 3 h. (c) Autophosphorylation kinetics. EL362 (R150G) (filled circles, dark state; open squares, lit state) has overall higher activity than EL362 (filled triangles). (d) SEC-MALLS shows that wild-type EL362 (monomer MW: 40.7 kDa) is predominantly monomeric in solution (MALLS trace ∼50 kDa at the center of the peak). Upon restoration of cofactor binding by the R150G point mutation, we observed oligomerization (MALLS MW ∼120 kDa in the dark, ∼100 kDa in the light) with some light-dependent effects on elution peak shape and molecular weight distribution (wild-type vs mutant). dRI and MW data are shown as described in Figure 2.

RRs, perhaps specifying their selection by the LOV-HKs (Figure S7A, Supporting Information). On the complementary HK surface, we observe sequence similarities among the DHp regions (Figure S7B, Supporting Information) as well as differences that may contribute to the differential phosphorylation levels of RR substrates.

Our findings suggest the existence of a complex light-regulated branched pathway in *E. litoralis* involving "many-to-one" (EL346, EL362, and EL368 with EL_LovR) and "one-to-many" (EL368 and EL346 with EL_LovR and EL_PhyR) HK and RR relationships. "Many to one" relationships allow the cell to integrate multiple inputs into the phosphorylation levels of a specific RR and consequently undergo appropriate physiological answers for each level.[38] EL368 and EL346 both feed into the same EL_LovR and EL_PhyR pathway; this apparent redundancy may be explained by either functional importance (e.g., different sensors have differential sensitivity to light) or simply a lack of selective pressure against keeping multiple LOV-HK proteins in the genome. We also note that this redundancy provides some robustness in the event of inactivation of one sensor, as perhaps seen by EL368 and EL346 compensating for the impaired function of the noninducible EL362 kinase (Figure 7). We speculate that perhaps EL362 may actually represent a genetic relic of sorts by having served as the ancestral light sensor in this organism (in a conventional operon arrangement with its cognate RR) prior to having suffered an inactivating mutation in its LOV domain. While rigorous testing of the potential *in vivo* roles of multiple LOV-HK proteins will require future experimental validation, we note this redundancy is not restricted solely to *E. litoralis*: multiple eubacteria (including several *Methylobacterium* species) contain two or more LOV-HK genes.

An additional degree of complexity ("one to many" relationship) is added to the transduction pathway by the ability of EL368/EL346 to phosphorylate EL_PhyR in addition to EL_LovR. Our biochemical analyses of EL_PhyR allow us to classify it as a PhyR-like response regulator; an analogous protein in *Methylobacterium extorquens* AM1 (which contains multiple LOV-HK proteins, see above) participates in the regulation of σ anti-σ interaction system, which is involved in resistance to multiple environmental stresses through the activation of several target genes.[20,21] Interestingly, Foreman et

dx.doi.org/10.1021/bi400617y | *Biochemistry* 2013, 52, 4656−4666

al. demonstrated that transcription of the LovK-LovR operon in *C. crescentus* is upregulated by the same general stress σ factor.[16] In *E. litoralis*, there is no direct evidence that EL368 and EL346 could be regulated by the σ factor. However, analysis of the intergenic region prior to the potential EL362-EL_LovR operon indicates the presence of a putative operator (**GGAACT** CCG AGC CGC TCA GTC **GGTT**) for the σ binding located 83 nucleotides prior to the start codon of the EL362 gene (designated by the EL_sigT promoter in Figure S8 (Supporting Information)), suggesting that *E. litoralis* may adopt a system of regulation similar to that observed in the related alphaproteobacterium *C. crescentus*. Nevertheless, we do observe some differences between *C. crescentus* and *E. litoralis*, particularly in the latter use of "orphan" HKs to phosphorylate RR proteins distant in the genome (i.e., EL368 and EL346 with EL_PhyR, EL_LovR). Notably, this allows *E. litoralis* to have a light-regulated network architecture similar to that observed in *C. crescentus*[16] despite the inability of native EL362 to be controlled by illumination.

In conclusion, our findings indicate the discovery of a light-regulated branched transduction pathway involving a set of several LOV-HKs and stress-related RRs. Additional biochemical and structural studies of these proteins would not only help to understand the molecular mechanisms of activation of HKs but also enhance our knowledge about the complexity and diversity of two-component signaling systems.

■ ASSOCIATED CONTENT

Supporting Information

Photokinetics of the dark state recovery of EL368 (Figure S1), secondary structure and domains disposition along EL368 sequence (Figure S2), phosphotransfer profiling of EL346 (Figure S3), chromosomal organization of the region containing EL362 and phosphotransfer of EL362 to EL_LovR (Figure S4), sequence alignment between EL368 and EL362 (Figure S5), sequence alignment among EL362 and other LOV-containing proteins highlighting the region containing the Gly to Arg substitution in EL362 (Figure S6), sequence alignment among *E. litoralis* RR proteins and additional alignment of HK DHp regions (Figure S7), comparison of light and stress-response regulatory systems between *E. litoralis* and *C. crescentus* (Figure S8), and the predicted response regulators from *E. litoralis* HTCC2594 (Table S1). This material is available free of charge via the Internet at http://pubs.acs.org.

■ AUTHOR INFORMATION

Corresponding Author

*Phone: 214-645-6365. E-mail: Kevin.Gardner@UTSouthwestern.edu.

Funding

We gratefully acknowledge funding from the NIH (R01 GM081875 to K.H.G.; T32 AI007520 supporting V.O.), NSF (0843662 to R.A.B.), and Robert A. Welch Foundation (I-1424 to K.H.G.) in support of this research.

Notes

The authors declare no competing financial interest.

■ ACKNOWLEDGMENTS

We thank Trevor Swartz for materials and discussions at the outset of this project, Giomar Rivera-Cancel for comments on this manuscript, and all the members of the Gardner Laboratory for helpful discussions.

■ ABBREVIATIONS USED

LOV domain, light oxygen voltage domain; HK, histidine kinase; RR, response regulator; dRI, differential refractive index; MALLS, multiangle laser light scattering

■ REFERENCES

(1) Stock, A. M., Robinson, V. L., and Goudreau, P. N. (2000) Two-component signal transduction. *Annu. Rev. Biochem. 69*, 183−215.

(2) Capra, E. J., and Laub, M. T. (2012) Evolution of two-component signal transduction systems. *Annu. Rev. Microbiol. 66*, 325−347.

(3) Herrou, J., and Crosson, S. (2011) Function, structure and mechanism of bacterial photosensory LOV proteins. *Nat. Rev. Microbiol. 9*, 713−723.

(4) Losi, A., and Gartner, W. (2012) The evolution of flavin-binding photoreceptors: an ancient chromophore serving trendy blue-light sensors. *Annu. Rev. Plant Biol. 63*, 49−72.

(5) Henry, J. T., and Crosson, S. (2011) Ligand-binding PAS domains in a genomic, cellular, and structural context. *Annu. Rev. Microbiol. 65*, 261−286.

(6) Salomon, M., Christie, J. M., Knieb, E., Lempert, U., and Briggs, W. R. (2000) Photochemical and mutational analysis of the FMN-binding domains of the plant blue light receptor, phototropin. *Biochemistry 39*, 9401−9410.

(7) Zoltowski, B. D., Vaccaro, B., and Crane, B. R. (2009) Mechanism-based tuning of a LOV domain photoreceptor. *Nat. Chem. Biol. 5*, 827−834.

(8) Harper, S. M., Christie, J. M., and Gardner, K. H. (2004) Disruption of the LOV-Jalpha helix interaction activates phototropin kinase activity. *Biochemistry 43*, 16184−16192.

(9) Harper, S. M., Neil, L. C., Day, I. J., Hore, P. J., and Gardner, K. H. (2004) Conformational changes in a photosensory LOV domain monitored by time-resolved NMR spectroscopy. *J. Am. Chem. Soc. 126*, 3390−3391.

(10) Vaidya, A. T., Chen, C. H., Dunlap, J. C., Loros, J. J., and Crane, B. R. (2011) Structure of a light-activated LOV protein dimer that regulates transcription. *Sci. Signaling 4*, ra50.

(11) Crosson, S., Rajagopal, S., and Moffat, K. (2003) The LOV domain family: photoresponsive signaling modules coupled to diverse output domains. *Biochemistry 42*, 2−10.

(12) Purcell, E. B., Siegal-Gaskins, D., Rawling, D. C., Fiebig, A., and Crosson, S. (2007) A photosensory two-component system regulates bacterial cell attachment. *Proc. Natl. Acad. Sci. U.S.A. 104*, 18241−18246.

(13) Cao, Z., Buttani, V., Losi, A., and Gartner, W. (2008) A blue light inducible two-component signal transduction system in the plant pathogen Pseudomonas syringae pv. tomato. *Biophys. J. 94*, 897−905.

(14) Swartz, T. E., Tseng, T. S., Frederickson, M. A., Paris, G., Comerci, D. J., Rajashekara, G., Kim, J. G., Mudgett, M. B., Splitter, G. A., Ugalde, R. A., Goldbaum, F. A., Briggs, W. R., and Bogomolni, R. A. (2007) Blue-light-activated histidine kinases: two-component sensors in bacteria. *Science 317*, 1090−1093.

(15) Losi, A. (2004) The bacterial counterparts of plant phototropins. *Photochem. Photobiol. Sci. 3*, 566−574.

(16) Foreman, R., Fiebig, A., and Crosson, S. (2012) The LovK-LovR two-component system is a regulator of the general stress pathway in *Caulobacter crescentus*. *J. Bacteriol. 194*, 3038−3049.

(17) Kraiselburd, I., Alet, A. I., Tondo, M. L., Petrocelli, S., Daurelio, L. D., Monzon, J., Ruiz, O. A., Losi, A., and Orellano, E. G. (2012) A LOV protein modulates the physiological attributes of *Xanthomonas axonopodis* pv. citri relevant for host plant colonization. *PLoS One 7*, e38226.

(18) Pathak, G. P., Losi, A., and Gartner, W. (2012) Metagenome-based screening reveals worldwide distribution of LOV-domain proteins. *Photochem. Photobiol. 88*, 107−118.

(19) Bonomi, H. R., Posadas, D. M., Paris, G., Carrica, M. D., Frederickson, M., Pietrasanta, L. I., Bogomolni, R. A., Zorreguieta, A., and Goldbaum, F. A. (2012) Light regulates attachment, exopolysaccharide production, and nodulation in *Rhizobium leguminosarum* through a LOV-histidine kinase photoreceptor. *Proc. Natl. Acad. Sci. U.S.A. 109*, 12135−12140.
(20) Francez-Charlot, A., Frunzke, J., Reichen, C., Ebneter, J. Z., Gourion, B., and Vorholt, J. A. (2009) Sigma factor mimicry involved in regulation of general stress response. *Proc. Natl. Acad. Sci. U.S.A. 106*, 3467−3472.
(21) Gourion, B., Francez-Charlot, A., and Vorholt, J. A. (2008) PhyR is involved in the general stress response of *Methylobacterium extorquens* AM1. *J. Bacteriol. 190*, 1027−1035.
(22) Oh, H. M., Giovannoni, S. J., Ferriera, S., Johnson, J., and Cho, J. C. (2009) Complete genome sequence of *Erythrobacter litoralis* HTCC2594. *J. Bacteriol. 191*, 2419−2420.
(23) Sheffield, P., Garrard, S., and Derewenda, Z. (1999) Overcoming expression and purification problems of RhoGDI using a family of "parallel" expression vectors. *Protein Expression Purif. 15*, 34−39.
(24) Amezcua, C. A., Harper, S. M., Rutter, J., and Gardner, K. H. (2002) Structure and interactions of PAS kinase N-terminal PAS domain: model for intramolecular kinase regulation. *Structure 10*, 1349−1361.
(25) Blommel, P. G., and Fox, B. G. (2007) A combined approach to improving large-scale production of tobacco etch virus protease. *Protein Expression Purif. 55*, 53−68.
(26) Karniol, B., and Vierstra, R. D. (2004) The HWE histidine kinases, a new family of bacterial two-component sensor kinases with potentially diverse roles in environmental signaling. *J. Bacteriol. 186*, 445−453.
(27) Moglich, A., Ayers, R. A., and Moffat, K. (2009) Design and signaling mechanism of light-regulated histidine kinases. *J. Mol. Biol. 385*, 1433−1444.
(28) Surette, M. G., Levit, M., Liu, Y., Lukat, G., Ninfa, E. G., Ninfa, A., and Stock, J. B. (1996) Dimerization is required for the activity of the protein histidine kinase CheA that mediates signal transduction in bacterial chemotaxis. *J. Biol. Chem. 271*, 939−945.
(29) Kenney, L. J. (1997) Kinase activity of EnvZ, an osmoregulatory signal transducing protein of *Escherichia coli*. *Arch. Biochem. Biophys. 346*, 303−311.
(30) Sousa, E. H., Gonzalez, G., and Gilles-Gonzalez, M. A. (2005) Oxygen blocks the reaction of the FixL-FixJ complex with ATP but does not influence binding of FixJ or ATP to FixL. *Biochemistry 44*, 15359−15365.
(31) Tawa, P., and Stewart, R. C. (1994) Kinetics of CheA autophosphorylation and dephosphorylation reactions. *Biochemistry 33*, 7917−7924.
(32) Yang, Y., and Inouye, M. (1991) Intermolecular complementation between two defective mutant signal-transducing receptors of *Escherichia coli*. *Proc. Natl. Acad. Sci. U.S.A. 88*, 11057−11061.
(33) Ninfa, E. G., Atkinson, M. R., Kamberov, E. S., and Ninfa, A. J. (1993) Mechanism of autophosphorylation of *Escherichia coli* nitrogen regulator II (NRII or NtrB): trans-phosphorylation between subunits. *J. Bacteriol. 175*, 7024−7032.
(34) Casino, P., Rubio, V., and Marina, A. (2009) Structural insight into partner specificity and phosphoryl transfer in two-component signal transduction. *Cell 139*, 325−336.
(35) Purcell, E. B., McDonald, C. A., Palfey, B. A., and Crosson, S. (2010) An analysis of the solution structure and signaling mechanism of LovK, a sensor histidine kinase integrating light and redox signals. *Biochemistry 49*, 6761−6770.
(36) Cole, C., Barber, J. D., and Barton, G. J. (2008) The Jpred 3 secondary structure prediction server. *Nucleic Acids Res. 36*, W197−201.
(37) Jentzsch, K., Wirtz, A., Circolone, F., Drepper, T., Losi, A., Gartner, W., Jaeger, K. E., and Krauss, U. (2009) Mutual exchange of kinetic properties by extended mutagenesis in two short LOV domain proteins from *Pseudomonas putida*. *Biochemistry 48*, 10321−10333.
(38) Laub, M. T., and Goulian, M. (2007) Specificity in two-component signal transduction pathways. *Annu. Rev. Genet. 41*, 121−145.
(39) Whitworth, D. E., and Cock, P. J. (2009) Evolution of prokaryotic two-component systems: insights from comparative genomics. *Amino Acids 37*, 459−466.
(40) Laub, M. T., Biondi, E. G., and Skerker, J. M. (2007) Phosphotransfer profiling: systematic mapping of two-component signal transduction pathways and phosphorelays. *Methods Enzymol. 423*, 531−548.
(41) Galperin, M. Y. (2006) Structural classification of bacterial response regulators: diversity of output domains and domain combinations. *J. Bacteriol. 188*, 4169−4182.
(42) Bateman, A., Coin, L., Durbin, R., Finn, R. D., Hollich, V., Griffiths-Jones, S., Khanna, A., Marshall, M., Moxon, S., Sonnhammer, E. L., Studholme, D. J., Yeats, C., and Eddy, S. R. (2004) The Pfam protein families database. *Nucleic Acids Res. 32*, D138−141.
(43) Gourion, B., Rossignol, M., and Vorholt, J. A. (2006) A proteomic study of *Methylobacterium extorquens* reveals a response regulator essential for epiphytic growth. *Proc. Natl. Acad. Sci. U.S.A. 103*, 13186−13191.
(44) Herrou, J., Rotskoff, G., Luo, Y., Roux, B., and Crosson, S. (2012) Structural basis of a protein partner switch that regulates the general stress response of alpha-proteobacteria. *Proc. Natl. Acad. Sci. U.S.A. 109*, E1415−1423.
(45) Campagne, S., Damberger, F. F., Kaczmarczyk, A., Francez-Charlot, A., Allain, F. H., and Vorholt, J. A. (2012) Structural basis for sigma factor mimicry in the general stress response of Alphaproteobacteria. *Proc. Natl. Acad. Sci. U.S.A. 109*, E1405−1414.
(46) Jenal, U., and Galperin, M. Y. (2009) Single domain response regulators: molecular switches with emerging roles in cell organization and dynamics. *Curr. Opin. Microbiol. 12*, 152−160.
(47) Delgado, J., Forst, S., Harlocker, S., and Inouye, M. (1993) Identification of a phosphorylation site and functional analysis of conserved aspartic acid residues of OmpR, a transcriptional activator for ompF and ompC in *Escherichia coli*. *Mol. Microbiol. 10*, 1037−1047.
(48) Nash, A. I., McNulty, R., Shillito, M. E., Swartz, T. E., Bogomolni, R. A., Luecke, H., and Gardner, K. H. (2011) Structural basis of photosensitivity in a bacterial light-oxygen-voltage/helix-turn-helix (LOV-HTH) DNA-binding protein. *Proc. Natl. Acad. Sci. U.S.A. 108*, 9449−9454.
(49) Zoltowski, B. D., and Crane, B. R. (2008) Light activation of the LOV protein vivid generates a rapidly exchanging dimer. *Biochemistry 47*, 7012−7019.
(50) Jurk, M., Dorn, M., Kikhney, A., Svergun, D., Gartner, W., and Schmieder, P. (2010) The switch that does not flip: the blue-light receptor YtvA from *Bacillus subtilis* adopts an elongated dimer conformation independent of the activation state as revealed by a combined AUC and SAXS study. *J. Mol. Biol. 403*, 78−87.
(51) Moglich, A., Ayers, R. A., and Moffat, K. (2009) Design and signaling mechanism of light-regulated histidine kinases. *J. Mol. Biol. 385*, 1433−1444.
(52) Moglich, A., Ayers, R. A., and Moffat, K. (2010) Addition at the molecular level: signal integration in designed Per-ARNT-Sim receptor proteins. *J. Mol. Biol. 400*, 477−486.
(53) Diensthuber, R. P., Bommer, M., Gleichmann, T., and Moglich, A. (2013) Full-length structure of a sensor histidine kinase pinpoints coaxial coiled coils as signal transducers and modulators. *Structure,*.
(54) Wang, C., Sang, J., Wang, J., Su, M., Downey, J. S., Wu, Q., Wang, S., Cai, Y., Xu, X., Wu, J., Senadheera, D. B., Cvitkovitch, D. G., Chen, L., Goodman, S. D., and Han, A. (2013) Mechanistic insights revealed by the crystal structure of a histidine kinase with signal transducer and sensor domains. *PLoS Biol. 11*, e1001493.
(55) Lupas, A., Van Dyke, M., and Stock, J. (1991) Predicting coiled coils from protein sequences. *Science 252*, 1162−1164.
(56) van der Horst, M. A., Key, J., and Hellingwerf, K. J. (2007) Photosensing in chemotrophic, non-phototrophic bacteria: let there be light sensing too. *Trends Microbiol. 15*, 554−562.

(57) Rivera-Cancel, G., Motta-Mena, L. B., and Gardner, K. H. (2012) Identification of natural and artificial DNA substrates for light-activated LOV-HTH transcription factor EL222. *Biochemistry 51*, 10024−10034.
(58) Avila-Perez, M., Hellingwerf, K. J., and Kort, R. (2006) Blue light activates the sigmaB-dependent stress response of *Bacillus subtilis* via YtvA. *J. Bacteriol. 188*, 6411−6414.
(59) Skerker, J. M., Perchuk, B. S., Siryaporn, A., Lubin, E. A., Ashenberg, O., Goulian, M., and Laub, M. T. (2008) Rewiring the specificity of two-component signal transduction systems. *Cell 133*, 1043−1054.
(60) Yamada, S., Sugimoto, H., Kobayashi, M., Ohno, A., Nakamura, H., and Shiro, Y. (2009) Structure of PAS-linked histidine kinase and the response regulator complex. *Structure 17*, 1333−1344.
(61) Szurmant, H., Bobay, B. G., White, R. A., Sullivan, D. M., Thompson, R. J., Hwa, T., Hoch, J. A., and Cavanagh, J. (2008) Co-evolving motions at protein-protein interfaces of two-component signaling systems identified by covariance analysis. *Biochemistry 47*, 7782−7784.
(62) Christie, J. M., Hitomi, K., Arvai, A. S., Hartfield, K. A., Mettlen, M., Pratt, A. J., Tainer, J. A., and Getzoff, E. D. (2012) Structural tuning of the fluorescent protein iLOV for improved photostability. *J. Biol. Chem. 287*, 22295−22304.